Effect of Governor Deadbands on Valve Travel using Long-Term Dynamic Simulation

Thad Haines and Matt Donnelly
School of Mines and Engineering
Montana Technological University
Butte, Montana 59701

***Abstract*—This paper investigates the impact of governor deadbands on valve travel using a novel long-term dynamic (LTD) simulation software environment. The Python based LTD software utilizes a commercial power-flow solver to execute a sequence of power flows that is shown to capture long-term power system dynamics with acceptable accuracy. While classical transient stability simulation (CTSS) is sufficient for investigating the impact of governor deadbands on primary frequency response, LTD software is needed for analyzing the impact of governor deadbands on fuel valve travel over longer periods of time. The presented LTD software enables simulations from tens of minutes to hours on full system base cases. Cumulative valve travel is proposed as a metric for evaluating the impact of various deadband settings. It is shown that use of specific governor deadbands can actually increase cumulative valve travel over what would be expected without a deadband.**

***Index Terms*—Governor deadband, long-term dynamic simulation, time-sequenced power flow, valve travel**

I. Introduction

Turbine speed governors commonly implement deadbands to prevent a machine from responding to small frequency deviations that are ever present in electrical systems. The North American Electric Reliability Corporation (NERC) has shown benefits of modifying governor deadbands in [2]. The Federal Energy Regulatory Commission (FERC) has adopted NERC deadband recommendations from [2] as FERC Order 842[6]. Industry usage of deadbands is widely known, however, it is often overlooked in power system simulation. Incorporating governor deadbands into classical transient stability simulation (CTSS) models has been shown to generate results that better match measured power system events[1]. While CTSS is useful for the study of deadband impact on primary frequency response, there is little understanding of the impact governor deadbands may have in the long-term. Because CTSS is focused on the millisecond to multiple minute time frame, the development of a simulation environment capable of simulating tens of minutes to hours is required. Long-term dynamic (LTD) simulation software has been proposed in [3]–[5], but has yet to be standardized or fully developed. The use of a single swing equation, as proposed in [3] and [5], for solving the equations of motion involved with an aggregated system inertia has been shown to produce an acceptable aggregate system frequency. In this work, the authors take this concept further to enable the study of governor deadbands over a much longer simulation time frame than can be reasonably accomplished with CTSS.

This paper explores the impact of governor deadbands using a novel LTD simulation environment based on GE Energy's Positive Sequence Load Flow (PSLF) system models, dynamic data, and load flow solver. Valve travel as a metric for comparing the impact of various deadband scenarios is proposed. Section II describes the LTD simulation environment used to perform the studies while Section III discusses governor and deadband modeling within the simulation environment. In Section IV, the LTD simulation is validated against industry standard CTSS. Finally, Section V presents some initial results demonstrating the viability of the proposed valve travel metric and Section VI offers conclusions.

II. Long-Term Dynamic Simulation Technique

Time-sequenced power flow (TSPF) is a method for LTD simulation proven to generate useful results[4]. The basic idea behind TSPF is to solve a power flow, calculate system dynamics of interest independent of the power-flow solver, 're-seed' the power flow with new values, and repeat. A Python based simulation software, Power System Long-Term Dynamic Simulator (PSLTDSim), has been developed to perform LTD simulations using TSPF. PSLTDSim has the ability to calculate system frequency, perform governor dynamics, model automatic generation control (AGC), and insert step, ramp, and noise type perturbances into a power system.

A. Simulation Assumptions and Simplifications

Due to the relatively large time steps of 1 second used with TSPF, numerous assumptions can be made. Ideal exciters were assumed as modern exicters are typically fast enough to maintain reference voltage under stable conditions. Intermachine oscillations were ignored since the time resolution used is not fine enough to capture these phenomena.

Simplifications of CTSS models are used in PSLTDSim. The only parameters required to model a generator are the machine's rated MW, MVA base, and inertia. Additionally, a deadband modified tgov1 governor model, shown in Fig. 1, was created to model turbine speed governors.

B. Modeling the System-Wide Frequency Response

Instead of frequency being calculated for every bus, a combined swing equation is used to model only one system frequency. As shown in (1), $\dot{\omega}_{sys}$ is calculated using accelerating power from the entire system, $P_{accPU,sys}$, and total

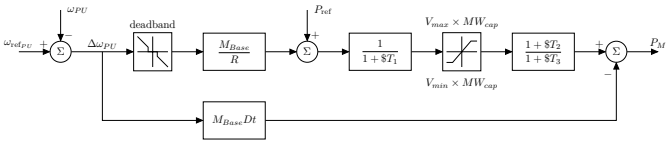

Fig. 1. Block diagram of modified tgov1 model.

system inertia $H_{PU,sys}$. An aggregate system frequency can then be found by integrating $\dot{\omega}_{sys}$.

$$\dot{\omega}_{sys} = \frac{1}{2H_{PU,sys}} \left(\frac{P_{accPU,sys}}{\omega_{sys}} - D_{sys}\Delta\omega_{sys} \right) \tag{1}$$

C. Distribution of Accelerating Power

In a system with N generators, total system accelerating power is calculated by

$$P_{acc,sys} = \sum_{i=1}^{N} P_{m,i} - \sum_{i=1}^{N} P_{e,i} \tag{2}$$

where $P_{m,i}$ is mechanical power and $P_{e,i}$ is electrical power of generator i.

System accelerating power is distributed to all generators in the system according to machine inertia as

$$P_{e,i} = P_{e,i} - P_{acc,sys} \left(\frac{H_i}{H_{sys}} \right) \tag{3}$$

where H has units of $MW \cdot s$.

The new value for $P_{e,i}$ is used in the next power flow solution for each generator. If the difference between expected and resulting power supplied by the slack generator is larger than a set slack tolerance, the difference is redistributed according to (3) until the resulting difference is below the slack tolerance, or a maximum number of iterations take place[5].

III. Implementation of Deadbands

FERC Order 842 specifies a droop of 5% and governor deadbands of a maximum 36 mHz[6]. In practice, several types of deadbands are currently used as physical control implementation is left to generator operators.

A. Types of Deadbands

Fig. 2 presents implementations of deadbands that meet FERC specifications. If a governor has no deadband, a change in output power is requested for any frequency deviation. A step deadband ignores any frequency smaller than the setpoint $\pm db_1$ and then steps to meet the set droop curve. A no-step deadband pushes the original droop curve away from the nominal frequency allowing for the droop curve to cross zero at $\pm db_2$ but never returns to the step or no deadband droop curve. A non-linear deadband is introduced that linearly increases from $\pm\alpha$ to $\pm\beta$, after which it follows the original droop curve.

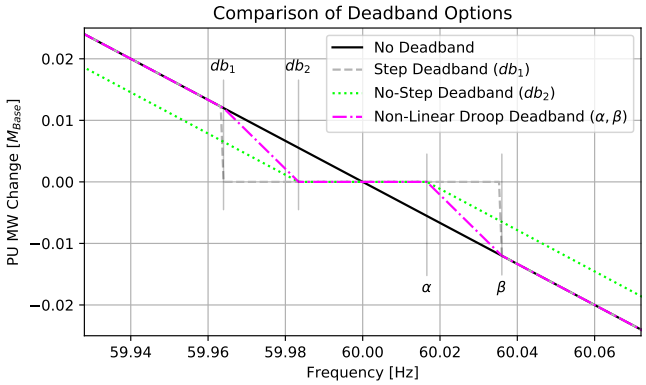

Fig. 2. Different types of deadbands.

IV. Simulation Validation

To validate the chosen simulation approach, identical system perturbations were simulated in both the PSLF Dynamic Subsystem (PSDS), an industry standard CTSS, and PSLTDSim. Frequency comparisons were used to validate the single system frequency assumption calculated by PSLTDSim. Comparisons of governed generator mechanical power were used to validate governor action.

Comparison of frequency data from PSDS to LTD was simplified by calculating a single weighted PSDS frequency f_w based on generator inertia. In a system with N generators

$$f_w = \sum_{i=1}^{N} f_i \frac{H_{PU,i} M_{base,i}}{H_{sys}} \tag{4}$$

$$\text{where } H_{sys} = \sum_{i=1}^{N} H_{PU,i} M_{base,i}. \tag{5}$$

A. The MiniWECC System

The power system used for validation and valve travel experiments, the 'miniWECC' shown in Fig. 3, is a 120 bus 34 generator system created in PSLF. The default miniWECC system was modified to include three areas for non-homogeneous deadband tests. All 21 governors in the miniWECC were modeled with the deadband modified tgov1 governor.More information about the creation and use of the miniWECC may be found in [7] and [8].

1) Load Step Results: A 400 MW load step at t = 2 seconds was used for validating the performance of the PSLTDSim. As shown in Fig. 4, all individual PSDS frequencies begin to oscillate after the perturbance while the weighted PSDS frequency appears to follow the general center of oscillation. The LTD system frequency is less oscillatory than the weighted frequency with only minor differences between the two. Fig. 9 quantifies these frequency differences.

When comparing mechanical power in Fig. 6, large MW differences can be seen, however, the percent difference data in Fig. 7 shows results less than 5% max difference, and an average percent difference of less than ≈0.5%.

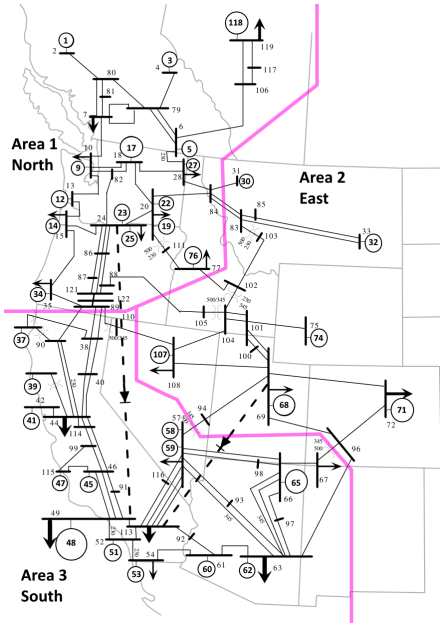

Fig. 3. MiniWECC system adapted from [7].

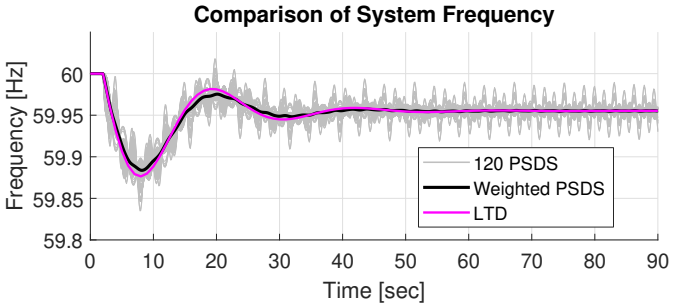

Fig. 4. Comparison of frequency during load step.

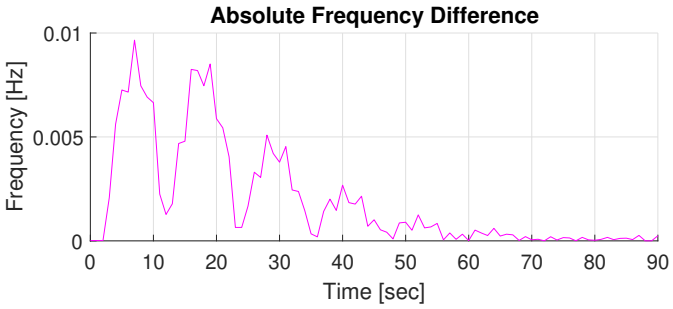

Fig. 5. Absolute difference of weighted frequency during load step.

2) Load Ramp Results: A second set of validation results, using a 40 second 400 MW load ramp, were also generated. Figs. 8-9 show frequency of LTD being within 1.5 mHz of PSDS. Fig. 10 shows mechanical power differences of less than ±10 MW or, as Fig. 11 shows, 1% difference max.

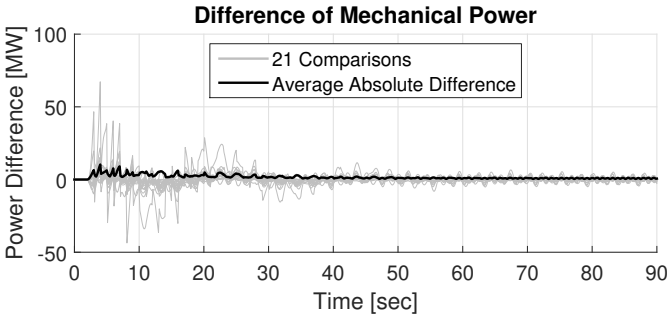

Fig. 6. Difference of mechanical power during load step.

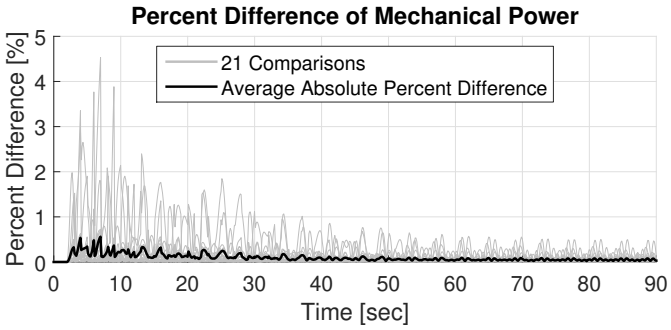

Fig. 7. Percent difference of mechanical power during load step.

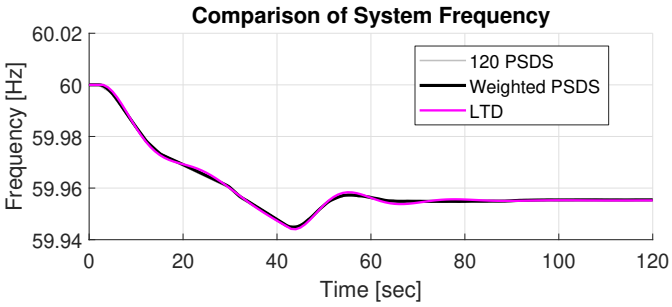

Fig. 8. Comparison of frequency during load ramp.

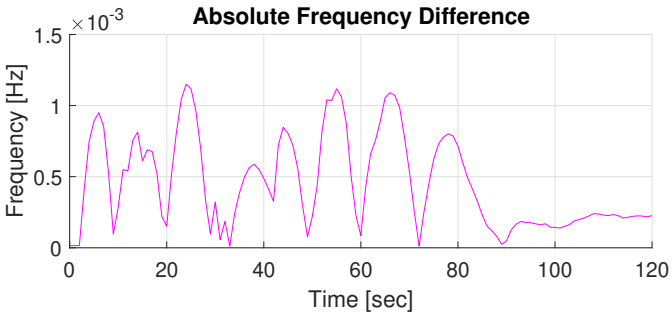

Fig. 9. Absolute difference of weighted frequency during load ramp.

B. Validation Summary

The validation results show that PSLTDSim accurately captures long-term power system dynamics. The step test results show that PSLTDSim cannot replace CTSS for the study

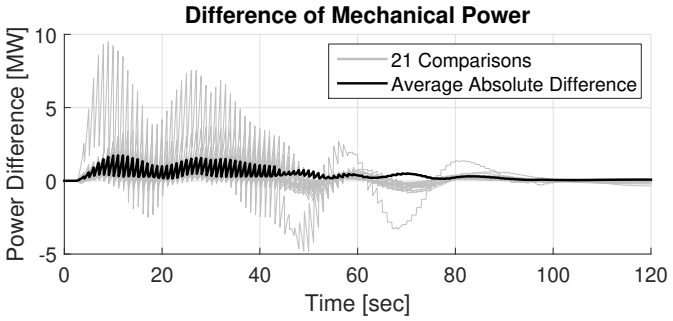

Fig. 10. Difference of mechanical power during load ramp.

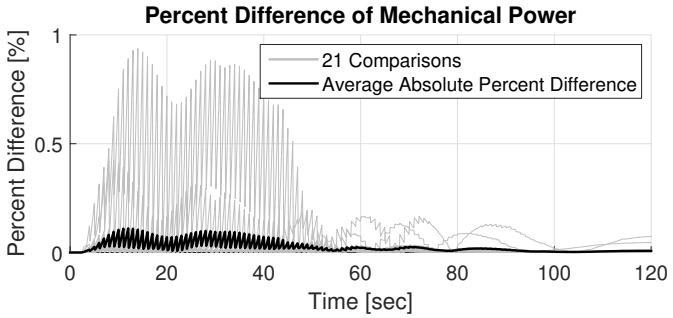

Fig. 11. Percent difference of mechanical power during load ramp.

of large, short-duration transient events. However, repeated small perturbances, such as those associated with ramps, are modeled with acceptable deviation from CTSS methods.

V. Initial Results

To assess long-term impacts of governor deadbands, thirty minutes of random load noise was applied to the miniWECC. All governors had identical deadband settings and PSLTDSim was used to set all governor droops to 5%. Some governors were removed from the system so that only ≈20% of generation capacity in each area had governor control. Each type of deadband shown in Fig. 2 was simulated.

Another experiment was conducted to explore a non-homogeneous deadband scenario where all deadbands were the same type, but some had different mHz deadbands. Although PSLTDSim can model AGC, it was not enabled for any presented simulation.

A. System Noise Injection

At every time step, noise is injected into each load $P_{L,i}$ in the system according to

$$P_{L,i} = P_{L,i}(1 \pm N_Z Rand_i) \tag{6}$$

where N_Z represents the maximum amount of random noise to inject as a percent, and $Rand_i$ is a randomly generated number between 0 and 1 inclusive. The decision to add or subtract noise is chosen by another randomly generated number. As described in [3], (6) creates random walk behavior in load that is representative of real power systems.

B. Noise Simulation Results

N_Z was set to 0.03 for all simulations. The change in system loading caused by the noise is shown in Fig. 12. Fig. 13 shows the resulting system frequency for each type of deadband. The step deadband holds frequency almost exactly on the set deadband except when system loading decreases during minutes 7-11. The other deadband options maintain system frequency near their respective mHz setting until loading increases beyond a point near minute 17.

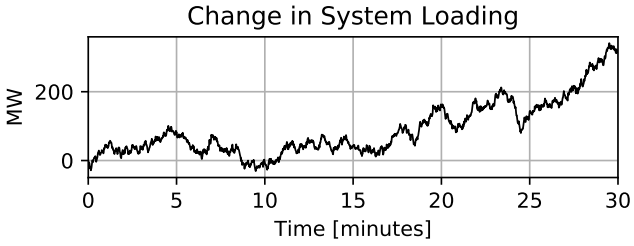

Fig. 12. Change in total system loading.

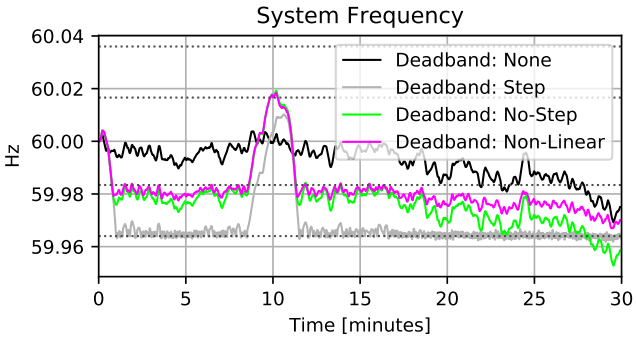

Fig. 13. System frequency response of various deadband scenarios.

Table I summarizes the valve travel for each generator in the system over the entire 30 minute simulation. A step type deadband has the largest total travel while the no-step deadband has the least.

TABLE I
Total valve travel for various deadband scenarios.

	Valve Travel [PU]				
Generator	No DB	Step	No-Step	N-L Droop	No-Step Non-H
17	0.16	7.48	0.15	0.23	0.19
23	0.16	7.48	0.15	0.23	0.19
30	0.16	7.48	0.15	0.23	0.19
32	0.16	7.54	0.15	0.23	0.19
107	0.16	7.54	0.15	0.23	0.19
41	0.15	6.44	0.14	0.23	0.06
45	0.15	6.44	0.14	0.23	0.06
53	0.16	7.54	0.15	0.23	0.06
59	0.15	6.44	0.14	0.23	0.06
Total:	1.41	64.38	1.32	2.07	1.19

The first three minutes of a single generators valve travel are shown in Fig. 14 to compare how different deadbands affect valve movement.

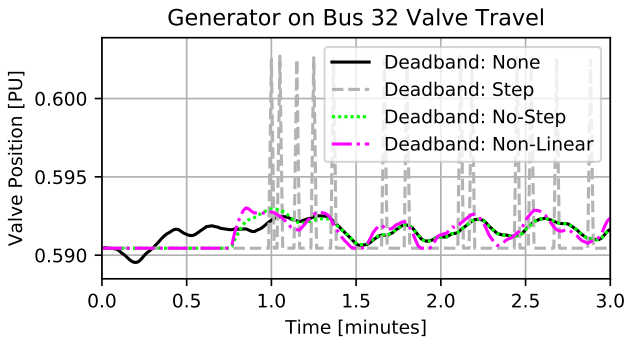

Fig. 14. Valve movement deadband comparisons.

A step deadband will send pulse train-esq control signals to the governor valve when system frequency is oscillating over the deadband. These repeated control pulses greatly increase valve travel over the more linear deadband options.

C. Non-Homogeneous Deadband Simulation Results

With all governors using a no-step type deadband, two of the three areas mHz deadband was to 16.6 mHz while the third was set to 36 mHz. The resulting system frequency is shown in Fig. 15. Individual valve travel for each generator is shown in Table I under the 'No-Step Non-H' column, and Fig. 16 shows the average valve travel over time for each area.

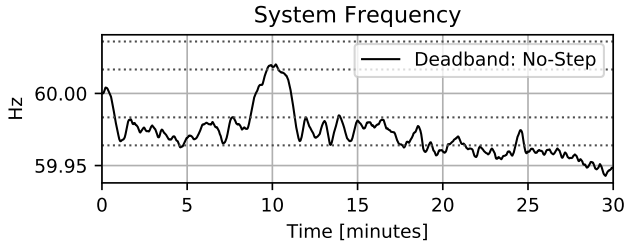

Fig. 15. System frequency response to 0.03% load noise where no-step deadbands have different settings.

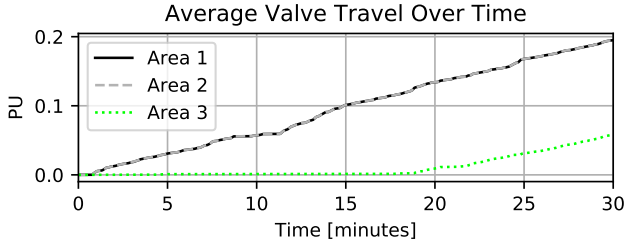

Fig. 16. Average valve travel by area for non-homogeneous deadband test.

As expected, governors with a larger deadband won't respond until after frequency drops below their deadband while governors with smaller deadbands work to maintain frequency. In this case, the governor valves with a smaller deadband move three times more than those with a larger deadband even though total system valve movement is reduced from the homogeneous no-step scenario.

VI. Conclusion

This work demonstrates that deadband configurations play a large role in dictating valve travel. Counterintuitively, a step deadband can lead to vastly increased valve travel compared to other deadband options. Smaller deadbands can reduce valve travel if adopted interconnection-wide, but in a system with various deadband settings, machines with smaller deadbands will respond more than machines with larger deadbands.

Further, this work demonstrates the need for a simulation environment that can capture long-term power system dynamics with appropriate static and dynamic models. The TSPF approach to LTD simulation that PSLTDSim utilizes is shown be be most useful. Future work in this area will focus on using the cumulative valve travel metric to study and optimize various governor and AGC control strategies.

Acknowledgment

This material is based upon work supported by the U.S. Department of Energy, Office of Science, Basic Energy Sciences, under Award Number DE-SC0012671.

References

[1] G. Kou, P. Markham, S. Hadley, T. King, and Y. Liu, "Impact of governor deadband on frequency response of u.s. eastern interconnection," IEEE Transactions on Smart Grid, 2016.

[2] NERC, "Frequency response initiative report," North American Electric Reliability Corporation, 2012.

[3] C. W. Taylor and R. L. Cresap, "Real-time power system simulation for automatic generation control," IEEE Transactions on Power Apparatus and Systems, 1976.

[4] E. Heredia, D. Kosterev, and M. Donnelly, "Wind hub reactive resource coordination and voltage control study by sequence power flow," IEEE, 2013.

[5] M. Stajcar, "Power system simulation using an adaptive modeling framework," Master's thesis, Montana Tech, 2016.

[6] FERC, "Essential reliability services and the evolving bulk-power system–primary frequency response," Federal Energy Regulatory Commission, Docket No. RM16-6-000 Order No. 842, Feb. 2018.

[7] D. Trudnowski, "Properties of the dominant inter-area modes in the wecc interconnect," Montana Tech, 2012.

[8] J. Sanchez-Gasca, M. Donnelly, R. Concepcion, A. Ellis, and R. Elliott, "Dynamic simulation over long time periods with 100% solar generation," Sandia National Laboratories, SAND2015-11084R, 2015.

[9] R. Hallett, "Improving a transient stability control scheme with wide-area synchrophasors and the microwecc, a reduced-order model of the western interconnect," Master's thesis, Montana Tech, 2018.